 FDMP, vol.14, no.2, pp.121-135, 2018

A Numerical Study of the Transitions of Laminar Natural Flows in a Square Cavity

Nouri Sabrina[1,] *, Abderrahmane Ghezal[1], Said Abboudi[2] and Pierre Spiteri[3]

Abstract: This paper deals with the numerical study of heat and mass transfer occurring in a cavity filled with a low Prandtl number liquid. The model includes the momentum, energy and mass balance equations. These equations are discretized by a finite volume technique and solved in the framework of a custom SIMPLER method developed in FORTRAN. The effect of the problem characteristic parameters, namely the Lewis and Prandtl numbers, on the instability of the flow and related solute distribution is studied for positive and negative thermal and solutal buoyancy forces ratio. Nusselt and Sherwood numbers are derived for values of the Prandtl number ranging between 10^{-2} and 10^{1} with the Lewis number spanning the interval $1\text{-}10^{4}$. The results show unicellular and multi-cellular flows featured by solute and kinematic boundary layers with thickness depending on the Prandtl number.

Keywords: Natural convection, low Prandtl number, heat and mass transfer, finite volume method, manuscript, preparation, typeset, format.

Nomenclature

Ar	aspect ratio
C	dimensionless concentration
D	solutal diffusion
G	gravitational acceleration m/s^2
Nu	Nusselt number
$\overline{Nu}$	average Nusselt number
P	dimensionless pressure
P_r	Prandtl number
Le	Lewis number
Ra	Rayleigh number
Sh	Sherwood number
$\overline{Sh}$	average Sherwood number
y	dimensionless vertical coordinate
z	dimensionless axial coordinate
ρ	density kg/m^3
α	thermal diffusivity m^2/s
β_T	coefficient of thermal expansion1/K
β_s	coefficient of solutal expansion 1/K
υ	kinematic viscosity m^2/s
ε	relative error
χ	stream function
Φ	global function

Subscripts

[1] Lmfta, the Department of Physics, usth, Bab Ezzouar, Algiers, Algeria.

[2] Utbm, Belfort-Montbéliard, France.

[3] Enseeiht-Toulouse, France.

* Corresponding Author: Nouri Sabrina. Email: Sabrina.nouri@gmail.com.

T dimensionless temperature
ΔT differenceof temperature°K
T dimensionless time
u dimensionless axial velocity
v dimensionless vertical velocity
x dimensionless axial coordinate

c cold wall
H hot wall
Ref reference
* dimensional form

1 Introduction

Natural convection of low-Prandtl-number fluids such as liquid metals is an important phenomenon often present in the production of industrial materials. For example, Bridgman crystal growth, floating zone and Heat exchanger methods. In these practical systems, inertial natural convection is dominant owing to low Prandtl number $\mathrm{Pr} \approx 0.01$ [Gelfgat (2001); Uspenskii and Favier (1994); Chiechun and Brown (1983)].

Many studies on crystal growth have been undertaken in the field of materials science [Yoshio, Akira, Yutaka et al. (2009); Kawaji, Gamache, Hwang et al. (2003); Lee and Chun (1999); de Vahl Davis (1983)]. Müller, Neumann and Weber et al. (1984) have studied experimentally and theoretically the naturalconvection in closed vertical cylinder heated from below. For various aspect ratios, they have investigated two different types of melts, H_2O (Pr=6.7), Ga and GaSb melts $\left(\mathrm{Pr} \approx 2 \times 10^{-2}\right)$. They have focused on the temperature profiles during growth. They showed clearly that the manifestation of doping striations in the GaSb crystals can be very well correlated with the unsteady flow regimes. Gelfgat and Bar-Yoseph [Gelfgat and Bar-Yoseph (2002)] have studied numerically the three-dimensional axisymmetry-breaking instability of convective flow during crystal growth from bulk. They considered a representative model of convection in a vertical cylinder with a parabolic temperature profile on the side wall.

Their main objective was the calculation of critical parameters corresponding to a transition from the steady axisymmetric to the three-dimensional non-axisymmetric oscillatory flow pattern. They showed the strong dependence of the critical Grashof number and the azimuthal periodicity on the resulting three-dimensional flow. Their results indicate the importance of a comprehensive parametric stability analysis in different crystal growth configurations. They suggest that a good understanding of oscillatory convection in liquid metals requires separate study in a more simplified geometrical system with a single body force. For this reason, we have turned to the classical Rayleigh-Bernard problem for low Prandtl numbers as described in the present paper.

Rayleigh-Bernard natural convection has been studied extensively but not for low Prandtl numbers. The oscillatory convection of molten semi-conducting materials has been known and considered as to be responsible for the undesirable strain in crystal rods. Fundamental studies on oscillatory convection are expected to clarify the general mechanism of oscillatory convection and suggest effective ways for its control. Some of the recent works on applications for material processing have been described by Lappa [Lappa (2007)]. Low Prandtl oscillatory natural convection numbers of fluids heated from a vertical side wall

[Pesso and Piva (2009)] or from below [Nakano and Ozoe (1998)] have also been studied. For example, Achoubir et al. [Achoubir, Bennacer, Cheddadi et al. (2008)] studied the effect of governing parameters, namely the Rayleigh number, the Lewis number and thermal to solutal ratio on the transition to oscillatory modes for thermal and solutal buoyancy forces. These forces oppose each other.

In the present study, we focus on the natural convection in a rectangular cavity filled with a metallic alloy characterized by a low Prandtl number. The results in terms of streamlines, isotherms, solute distribution, average Nusselt and Sherwood numbers are presented for a wide range of Lewis and Prandtl numbers.

Authors are encouraged to use the template for Microsoft Word, to prepare the final version of their manuscripts and facilitate typesetting. Authors may elect to submit two versions of their manuscript, one for the printed version of the journal, and the other for the on-line version of the journal. Illustrations in color are allowed only in the on-line version of the journal.

2 Physical problem and mathematical formulation

The physical model consists of two-dimensional rectangular enclosure heated from the left side and cooled from the right one. The temperatures T_h and Tc are maintained constant. The concentrations C_h at the left and the right walls are also considered constant. The cavity is filled with a fluid with Prandtl number $\left(10^{-2} \le \mathrm{Pr} \le 10\right)$. Fig. 1 depicts the system.

The fluid in the cavity is considered incompressible and Newtonian with negligible viscous dissipation. Furthermore, all thermos-physical properties of the fluid are constant except for the density variation in the buoyancy term. The density reads:

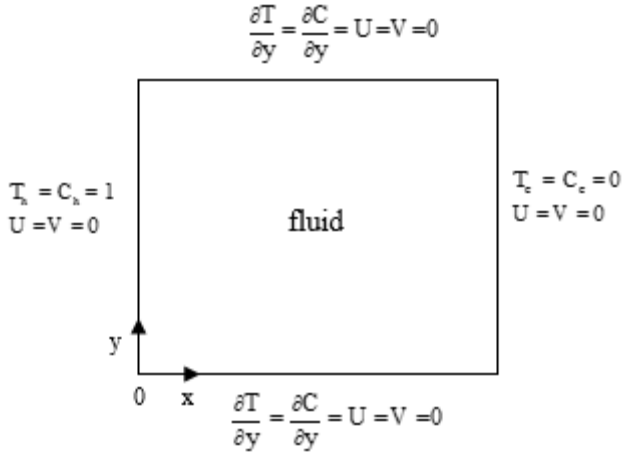

Figure 1: Physical system model and boundary conditions

$$\rho = \rho_{\mathrm{ref}}\left[1-\beta_{\mathrm{T}}\left(\mathrm{T}^{*}-\mathrm{T}_{\mathrm{ref}}\right)+\beta_{\mathrm{C}}\left(\mathrm{C}^{*}-\mathrm{C}_{\mathrm{ref}}\right)\right] \tag{1}$$

The dimensionless variables are:

$$x=\frac{x^*}{H},\ y=\frac{y^*}{H},\ u=\frac{u^*H}{\alpha},\ v=\frac{v^*H}{\alpha},\ T=\frac{\left(T^*-T_c\right)}{\left(T_h-T_c\right)},P=\frac{p^*H^2}{\rho\alpha^2},\ C=\frac{\left(C^*-C_c\right)}{\left(C_h-C_c\right)},\ t=\frac{\alpha t^*}{H^2}$$

The two-dimensional continuity and momentum equations coupled with the energy and solute transport equations under the Boussinesq approximation, may be now written in dimensionless form as follows:

$$\frac{\partial u}{\partial x}+\frac{\partial v}{\partial y}=0 \tag{2}$$

$$\frac{\partial u}{\partial t}+u\frac{\partial u}{\partial x}+v\frac{\partial u}{\partial y}=-\frac{\partial p}{\partial x}+Pr\left(\frac{\partial^2 u}{\partial x^2}+\frac{\partial^2 u}{\partial y^2}\right) \tag{3}$$

$$\frac{\partial v}{\partial t}+u\frac{\partial v}{\partial x}+v\frac{\partial v}{\partial y}=-\frac{\partial p}{\partial y}+Pr\left(\frac{\partial^2 v}{\partial x^2}+\frac{\partial^2 v}{\partial y^2}\right)+Ra\,Pr\left(T+NC\right) \tag{4}$$

$$\frac{\partial T}{\partial t}+u\frac{\partial T}{\partial x}+v\frac{\partial T}{\partial y}=\frac{\partial^2 T}{\partial x^2}+\frac{\partial^2 T}{\partial y^2} \tag{5}$$

$$\frac{\partial C}{\partial t}+u\frac{\partial C}{\partial x}+v\frac{\partial C}{\partial y}=\frac{1}{Le}\left(\frac{\partial^2 C}{\partial x^2}+\frac{\partial^2 C}{\partial y^2}\right) \tag{6}$$

The problem is governed by four dimensionless numbers: the thermal Rayleigh number $Ra=g\beta_T\left(T_H-T_C\right)H^3/\nu\alpha$, the Prandtl number $Pr=\nu/\alpha$, the Lewis number $Le=\alpha/D$ and the buoyancy ratio number $N=\beta_s\left(C_H-C_C\right)/\beta_T\left(T_H-T_C\right)$.

The boundary conditions correspond to various physical situations:

No-slip boundary conditions are specified at all walls. The temperature and concentration on the boundaries are given by:

for $y\in[0,1]$:

$$T(0,y)=T_h=0.5,\quad C(0,y)=C_h=0.5,\quad u(0,y)=v(0,y)=0$$

$$T(1,y)=T_c=-0.5,\quad C(1,y)=C_c=-0.5,\quad u(1,y)=v(1,y)=0$$

for $x\in[0,1]$

$$\frac{\partial T(x,0)}{\partial y}=\frac{\partial C(x,0)}{\partial y}=0\ ,\ \frac{\partial T(x,1)}{\partial y}=\frac{\partial C(x,1)}{\partial y}=0,\ u(x,0)=v(x,0)=0 \tag{7}$$

The Nusselt and Sherwood numbers characterizing, respectively, the dimensionless heat and mass transfer are defined by:

$$Nu=\int_{y=0}^{y=1}\left.\frac{\partial T}{\partial x}\right|_{x=1}dy \tag{8}$$

$$Sh = \int_{y=0}^{y=1} \left| \frac{\partial C}{\partial x} \right|_{x=1} dy \tag{9}$$

The stream function ψ is expressed by the following expressions:

$$u = \frac{\partial \psi}{\partial y}, \quad v = -\frac{\partial \psi}{\partial x} \tag{10}$$

3 Numerical method

Finite volume method has been used for spatial discretization. Note that the power-law scheme was adopted for the discretization of the convection-diffusion term. The temporal discretization is achieved using the explicit Euler time marching scheme with a time step Δt equal to 10^{-4}.The SIMPLER algorithm is used to solve the velocity-pressure coupling by Patankar [Patankar (1980)]. Thereafter, a line by line method is applied to solve the resulting system of linear algebraic equations. For all dependent variables u, v, T and C, the convergence criterion was set at a maximum relative error to be less than 10^{-4}; this statement corresponds to the relation:

$$\varepsilon = \text{Max} \left| \frac{\phi^{n+1} - \phi^{n}}{\phi^{n}} \right| \leq 10^{-4} \tag{11}$$

The mesh is constituted by an irregular sinusoidal distribution of nodes. A global mesh refinement was carried out. It consists on choosing between 40×40 to 120×120 grid points. Such choice of values of the discretization parameters allows an accurate description of the thermosolutal convection phenomena within the cavity for $Ra \prec 10^5$

4 Validation

The convergence of the numerical schema has been assumed through validation procedure against the results provided by Lage et al. [Lage and Bejan (1991); Erbay, Altaç and Sûlûs (2003); de Vahl Davis (1983); Morega and Nishimura (1998); Oueslati, BenBeya and Lili (2014)]. These results have been derived under the Boussinesq assumption. The comparison is summarized in Tab. 1. For $Pr \prec 10^{-2}$, a very good agreement between the present predictions and those provided by Lage et al. [Lage and Bejan (1991)] and Erbay et al. [Erbay, Altaç and Sûlûs (2003)] can be observed. For Pr = 0.71, $Ra=10^3$ and $Ra=10^6$ the present predictions are in a very good agreement with the data provided by de Vahl Davis [de Vahl Davis (1983)].

In the case of the natural double diffusive convection, the numerical code was validated with two cases of aspect and buoyancy ratio; the results are compared with those obtained by Morega et al. [Morega and Nishimura (1998); Oueslati, BenBeya and Lili (2014); Teamah (2008)] when Pr=1, Le=2 and $Ra=10^3$. Tab. 2 lists the average Nusselt and Sherwood numbers. Good agreements between the present computation and those of Morega et al. [Morega and Nishimura (1998); Oueslati, BenBeya and Lili (2014)] and Teamah [Teamah (2008)] are observed.

Table 1: The summary of the present and Benchmark results for steady-state Nusselt values

Pr	Ra	Lage and Bejan (1991)	Erbay, Altaç and Sûlûs (2003)	Grid	Present results
10^{-2}	10^2	1.00	1.004	40×40	1.001
	10^3	1.05	1.080	40×40	1.08
	10^4	1.50	1.593	40×40	1.593
	10^5	2.77	2.778	40×40	2.772
1	10^5	4.9	4.674	90×90	4.612
	10^6	9.2	9.194	100×100	8.975
	10^7	17.9	17.897	100×100	16.942

Table 2: Average Nusselt number compares with those of de Vahl Davis [de Vahl Davis (1983)] for $\mathrm{Pr} = 0.71,\ \mathrm{Ar} = 1$

Ra	Lage and Bejan (1991)	Present work	Mean deviation (%)
10^3	1.174	1.119	4.9
10^6	8.800	8.910	1.2

Table 3: Average Nusselt and Sherwood numbers compared with results found in Nishimura et al. [Nishimura, Wakamatsu and Morega (1998); Oueslati, BenBeya and Lili (2014)]

	Present work	Nishimura, Wakamatsu and Morega (1998)	Mean deviation (%)	Oueslati, BenBeya and Lili (2014)	Mean deviation (%)
$\overline{\mathrm{Nu}}$	3.0222	3.0100	0.40	3.0138	0.28
$\overline{\mathrm{Sh}}$	3.8336	3.82	0.36	3.8275	0.18

Table 4: Average Nusselt and Sherwood numbers compared with those of Oueslati et al. [Oueslati, BenBeya and Lili (2014)] and Teamah [Teamah (2008)] for $\mathrm{Pr} = 1,\ \mathrm{Le} = 2,\ \mathrm{Ra} = 10^5,\ \mathrm{N} = -0.8,\ \mathrm{Ar} = 2$

	Present work	Oueslati, BenBeya and Lili (2014)	Mean deviation (%)	Teamah (2008)	Mean deviation (%)
$\overline{\mathrm{Nu}}$	3.4178	3.3952	0.66	3.4613	1.2
$\overline{\mathrm{Sh}}$	4.3993	4.39170	0.17	4.37677	0.51

5 Results and discussion

In order to investigate the influence of the Prandtl and Lewis numbers on the flow and solute distribution, further computations have been carried out for different values of dimensionless parameters. The results of numerical simulations are summarized below:

a. The mesh refinement effect

Different mesh sizes were tested for $Pr = 10^{-2}, Le = 10^{4}$, $N = 5$ and $Ra = 10^{5}$ with the number of nodes ranging from 60×60 to 120×120. This allows determining the available grid size and shows the extensive grid independence of the numerical results for the considered problem. The corresponding results are given in Tab. 5. It is found that as soon as the grid gets finer than 100×100 , the flow intensity, represented by the stream function ψ_{max} and ψ_{min} and Nusselt number remains unaltered.

Table 5: Mesh indepence study for: $Pr = 10^{-2}, Le = 10^{4}$, $N = 5$, $Ra = 5 \times 10^{4}$, $Ar = 1$, $t = 1$, $\Delta t = 10^{-5}$

mesh	60×60	80×80	100×100	120×120
ψ_{min}	0.183	0.213	0.219	0.220
ψ_{max}	-5.366	-5.632	-5.835	-5.895
$\overline{Nu}$	2.403	2.431	2.457	2.457
$\overline{Sh}$	55.570	71.023	83.470	83.610

Fig. 2 shows that the mesh refinement has a large effect on the development of the boundary layer flow and on the solute boundary layer except for the temperature profile represented by isotherms which remains the same. Results presented in Tab. 5 show that the grid 100×100, or other finer alternatives, is sufficiently sharp to ensure a good development of the flow and solute boundary layers. In this case, the grid 100×100 ensures the mesh independent solution. Such grid size is sufficient to perform all subsequent computations and can be utilized in the numerical treatment of the current analysis.

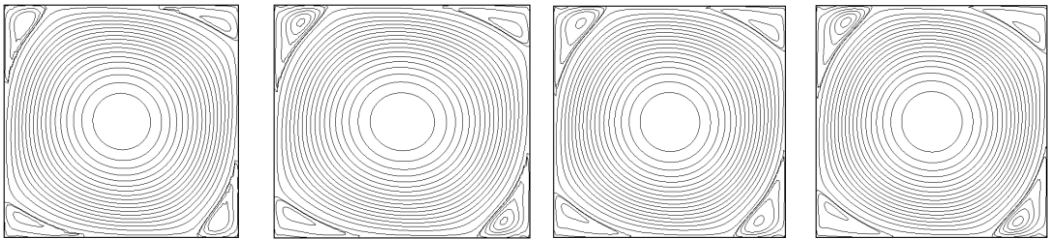

Streamlines

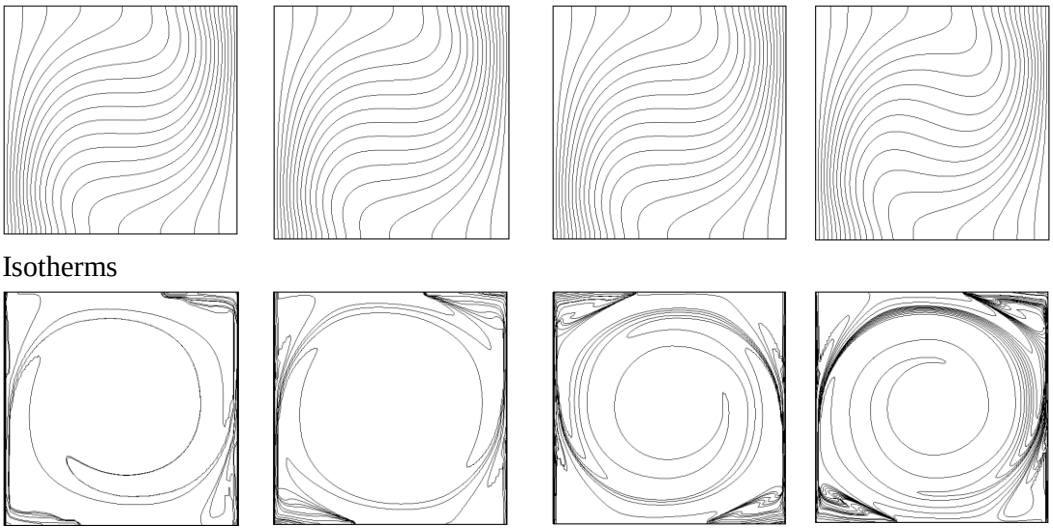

Figure 2: Effect of mesh on streamline patterns, isotherms and solute distribution for: $\mathrm{Pr}=10^{-2}, \mathrm{Le}=10^{4}$, $\mathrm{N}=5$, $\mathrm{Ra}=5\times10^{4}$, $\mathrm{Ar}=1$, $\Delta t=10^{-5}$

b. Numerical stability criterion independence testing

Numerical stability criteria have been considered. They consist on reaching stable values for the velocity, temperature and concentration. Tab. 6 depicts the flow intensity represented by the maximum and minimum stream function, the average Nusselt and Sherwood numbers calculated for various values of numerical the stability criterion. The effect of the stability criterion ε on the appearance of small cells at the vertical sides of the cavity appears clearly on Fig. 3 for $\varepsilon \le 10^{-5}$ when the solute boundary layer is well developed.

Tab. 7 shows that results in terms of stream function, average Nusselt and Sherwood numbers are not influenced by the time step values.

However, the Fig. 4 demonstrates that the evolution of the average Nusselt number throughout the time is well done for Δt equals to 10^{-5}. At the beginning of the period, the rate of heat transfer corresponding to $\Delta t = 10^{-2}$ is higher than for those of $\Delta t \prec 10^{-2}$ and this remains during all the time. In this case, the average Nusselt number has a constant value of 2.4. So the transition period is not visualized for $\Delta t = 10^{-2}$ and only the steady state can be noticed.

For $\Delta t = 10^{-5}$, the line graph starts from zero where no heat transfer rateat the hot wall of the cavity in the beginning of the period. Over time, the average Nusselt number increases significantly reaching the value of the steady state and remains constant. The transition period is well developed for $\Delta t \le 10^{-5}$. In the following calculations, the stability criterion ε of 10^{-5} and the time step $\Delta t = 10^{-5}$ are considered.

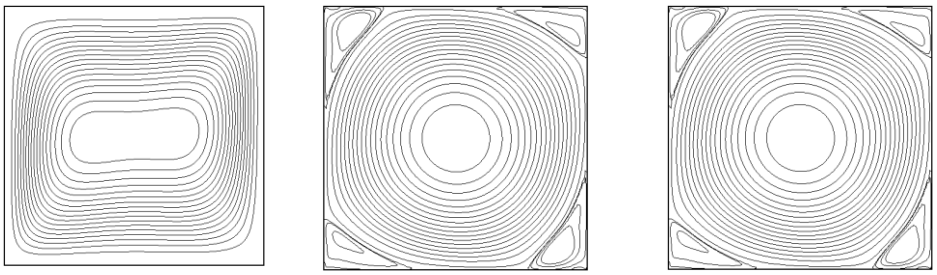

Streamlines

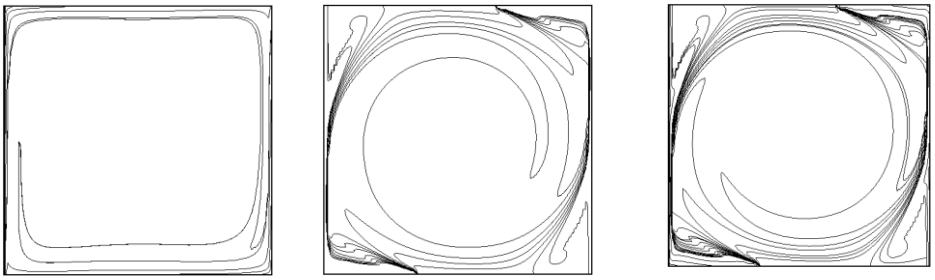

Isoconcentration lines

$\varepsilon = 10^{-2}$ $\varepsilon = 10^{-4}$ $\varepsilon = 10^{-6}$

Figure 3: Effect of convergence criterion on the flow structure and solute distribution for: $Pr = 10^{-2}, Le = 10^{4}, N = 5, Ra = 5 \times 10^{4}, Ar = 1, \Delta t = 10^{-5}$

Table 6: Convergence criterion independence study

$\varepsilon = Max\left\lvert\frac{\phi^{n+1}-\phi^{n}}{\phi^{n}}\right\rvert$	10^{-2}	10^{-3}	10^{-4}	10^{-5}	10^{-6}
ψ_{min}	-9.11	-5.805	-5.835	-5.835	-5.835
ψ_{max}	0	0.063	0.221	0.221	0.221
$\overline{Nu}$	3.828	2.554	2.457	2.457	2.457
$\overline{Sh}$	88.64	79.62	83.347	83.348	83.348

Table 7: Effect of time step study for: $Pr = 10^{-2}, Le = 10^{4}, N = 5, Ra = 5 \times 10^{4}, Ar = 1$

TIME STEP Δt	10^{-2}	10^{-3}	10^{-4}	10^{-5}
ψ_{max}	0.143	0.143	0.143	0.143
ψ_{min}	-5.125	-5.125	-5.125	-5.125
$\overline{Nu}$	2.401	2.401	2.401	2.401
$\overline{Sh}$	42.130	42.130	42.130	42.130

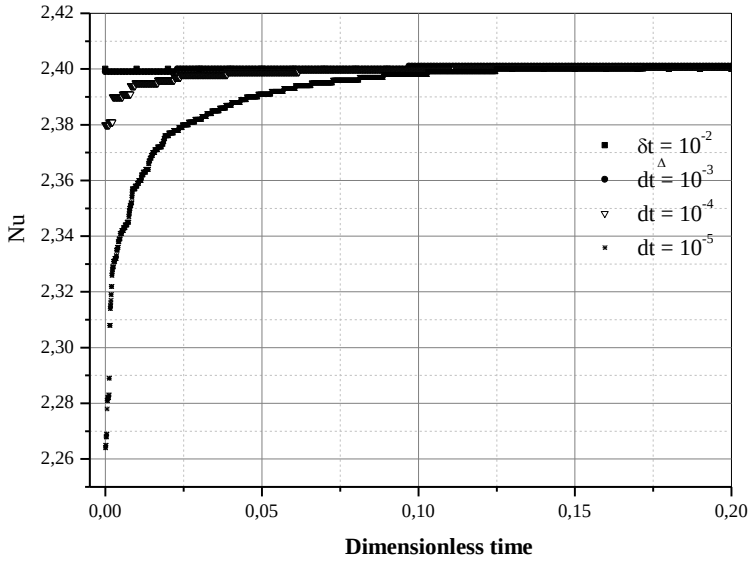

Figure 4: Average Nusselt evolutions for different values of time step

c. Effect of Lewis number

A computational analysis has been performed to investigate the effects of Lewis number on natural convection at low Prandtl number $\mathrm{Pr} = 0.01$. Fig. 5 shows the effect of Lewis number on streamline patterns, isotherms and iso-concentrations. Many multi cellular flow distributions are observed inside the cavity according to the Lewis number. In the case of stream lines for low Lewis number, the number of circular cells trends to increase [Mahfooz and Hossain (2012)]. As to the temperature distribution, convective distortion of isotherms occurs throughout the cavity due to the strong influence of the convective current in the cavity. It is obvious that flow increases with Lewis number; alike for iso-concentration distribution.

Fig. 6 illustrates that the Nusselt number declines over the increasing of the Lewis number, whereas the Sherwood number remains fixed. At low Lewis number value around 1, the Nusselt and Sherwood numbers are equal and their graph lines start from the same value.

It can be noticed that the Nusselt number increases at large values of Lewis number, while the Sherwood number remains fixed. Therefore, the Lewis number has generally no inhibiting effect on the Sherwood number.

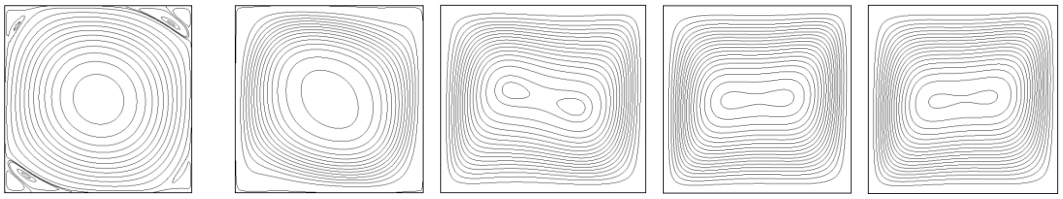

Streamlines

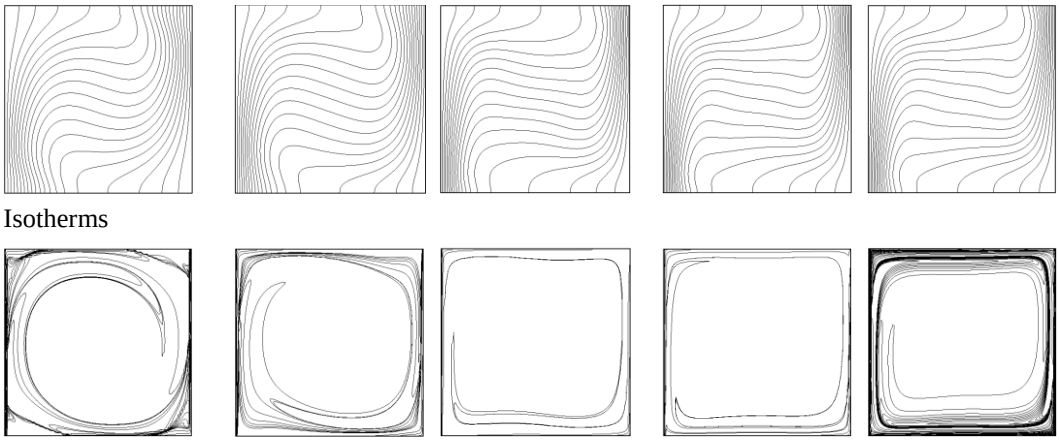

Figure 5: Effect of Lewis number on the flow structure, isotherms and solute distribution for: $Pr = 10^{-2}$, $N = 5$, $Ra = 5 \times 10^4$, $Ar = 1$, $\Delta t = 10^{-5}$

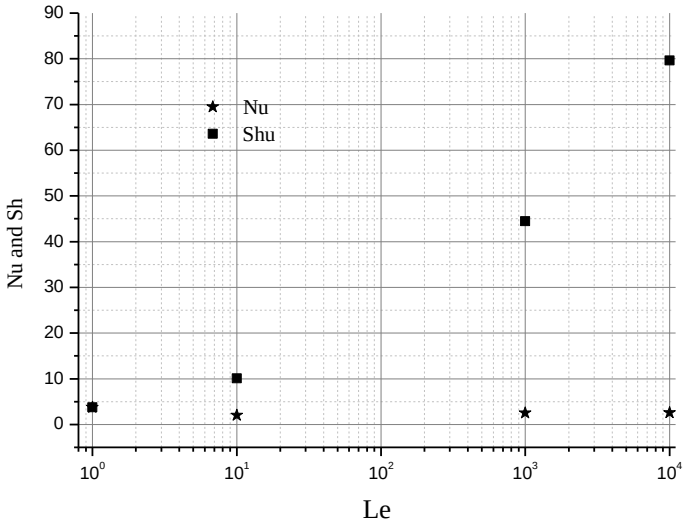

Figure 6: Effect of Lewis number on the average Nusselt and Sherwood numbers for: $Pr = 10^{-2}$, $N = 5$, $Ra = 5 \times 10^4$, $Ar = 1$, $\Delta t = 10^{-5}$

d. Effect of Prandtl number

Fig. 7 shows the isotherms, the iso-concentration and the streamlines of the roll cells circulation in the enclosure. The flow patterns and solute distributions are quite similar when $Pr \geq 10$. At low Prandtl number, the convective motion inside the enclosure becomes more active and produces secondary vortices at each corner of the enclosure. On the other hand, in the case of high Prandtl numbers, the flow around the body is quite stratified and contacts the top and bottom walls much more widely.

Fig. 8 shows the effect of Prandtl number on the average Nusselt and Sherwood numbers. The numerical results in the Fig. 8(a) indicate that the variation of the Nusselt number is very important for the Prandlt number between 0.01 and 20. For a Prandtl number greater than 25, the average Nusselt number does no longer depend on the Prandtl number and becomes constant. The Fig. 7(b) shows that the dependency of the mass transfer rate on the Prandtl number is important when the later is lower than 10. Otherwise Sherwood number remains constant.

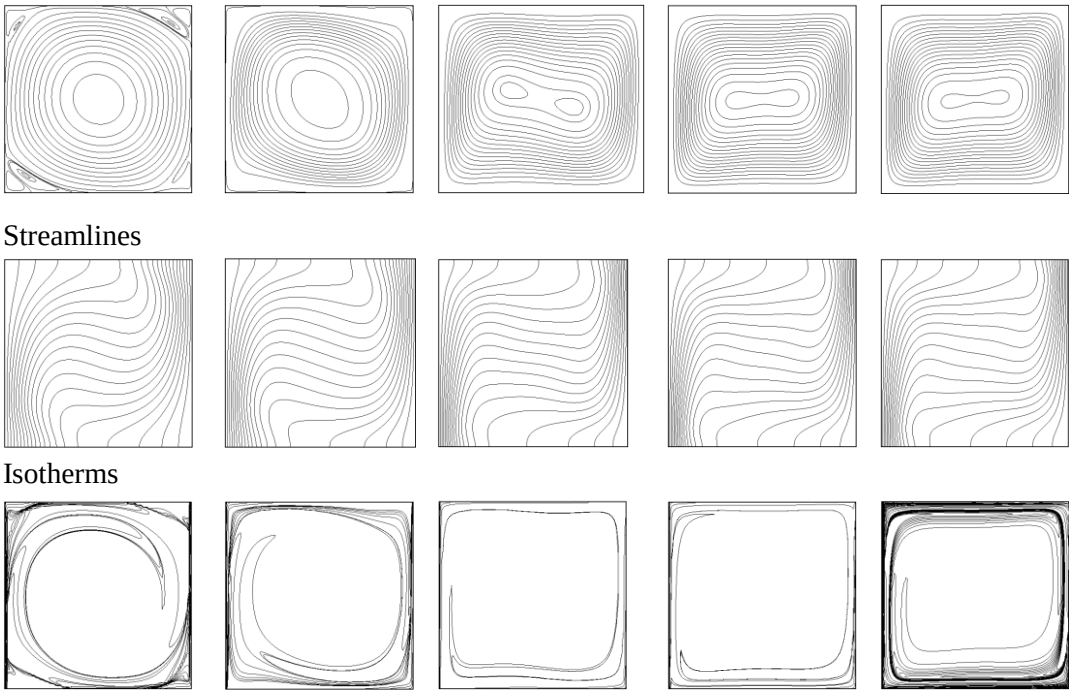

Figure 7: Effect of Prandtl number on the flow structure, isotherms and solute distribution for: $\mathrm{Le} = 10^4$, $\mathrm{N} = 5$, $\mathrm{Ra} = 5 \times 10^4$, $\mathrm{Ar} = 1$, $\Delta t = 10^{-5}$

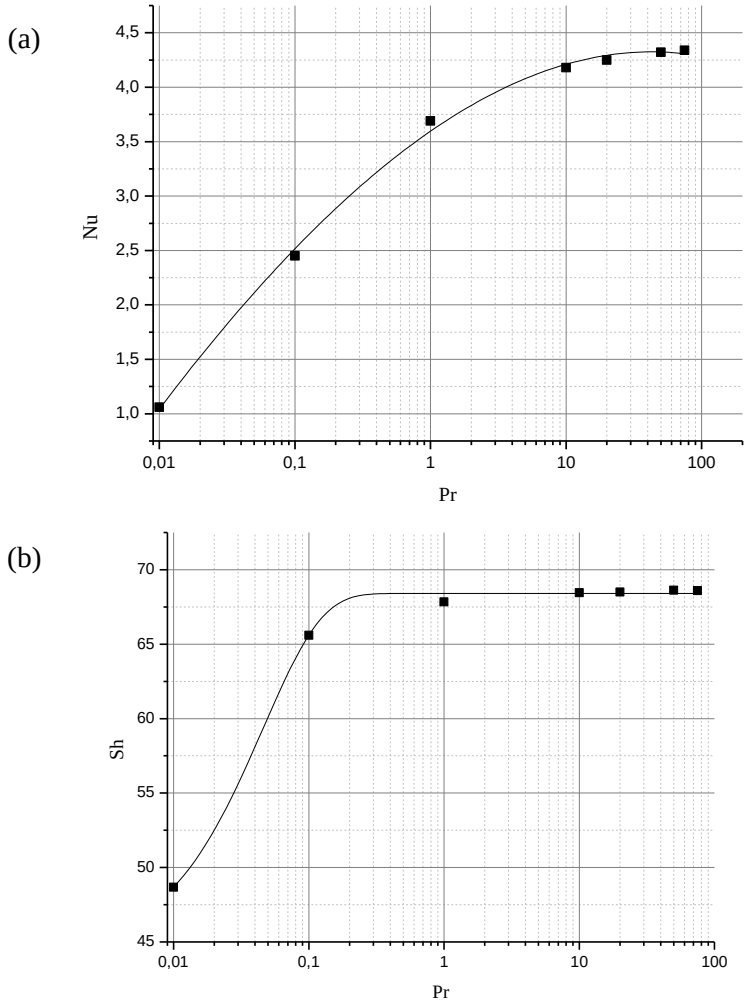

Figure 8: Effect of Prandtl number, (a) the average Nusselt, (b) Sherwood numbers $\mathrm{Le} = 10^4,\ \mathrm{N} = -5,\ \mathrm{Ra} = 5 \times 10^4,\ \mathrm{Ar} = 1$

6 Conclusions

The problem of natural convection, heat and mass transfer transitions in a rectangular enclosure has been studied numerically. Various Prandtl and Lewis numbers have been considered for the streamlines, the temperature field, the solute distribution and for Nusselt and Sherwood numbers. Rayleigh and buoyancy ratio numbers are kept constant.

The analysis of the numerical results leads to the following conclusions:

In steady state and for moderate Rayleigh number Ra values, the flow structure, the thermal field and the solute distribution depend strongly on the Prandtl and Lewis numbers.

The Nusselt and Sherwood numbers are in strong dependence on the low Prandtl number values $10^{-2} \le \mathrm{Pr} \le 10^{1}$

The Nusselt and Sherwood numbers for a high Prandtl number are larger than in cases of low Prandtl numbers,

The boundary layers in the flow field and solute distribution appear for the Prandlt number lower than 10^{-1}.

The effect of Lewis number on the flow, thermal field and solute distribution is also investigated. It is observed that the mass transfer rate increases with the Lewis number and that the multi-cell state to mono-cell state transition of the flow structures is obtained far from the vertical sides.

Acknowledgement: The authors wish to express their gratitude to PrF. SOUIDI member of our team "transfers and Entropy phenomena" of the laboratory LMFTA of the Houari Boumediene university USTHB for the precious help and the particular interest for this work. The authors would like to thank the respected reviewers for their valuable suggestions for improving the quality of the manuscript.

References

Achoubir, K.; Bennacer, R.; Cheddadi, A.; El Ganaoui, M.; Semma, E. (2008): Numerical study of thermosolutal convection in enclosures used for directional solidification (Bridgman cavity). *Fluid Dynamics & Materials Processing*, vol. 4, pp. 199-209.

Chang, C. J.; Robert Brown, A. (2003): Radial segregation induced by natural convection and melt/solid interface shape in vertical Bridgman growth. *International Journal of Crystal Growth*, vol. 63, pp. 343-364.

de Vahl Davis, G. (1983): Natural convection of air in a square cavity: A benchmark numerical solution. *International Journal for Numerical Methods in Fluids*, vol. 3, pp. 249-264.

Erbay, L.; Altaç, Z.; Sûlûs, B. (2003): An Analysis of the entropy generation in a square enclosure. *Entropy*, vol. 5, pp. 496-505.

Gelfgat, A. Y.; Bar-Yoseph, P. Z. (2002): Solan A. Axisymmetry breaking instabilities of natural convection in a vertical Bridgman growth configuration. *International Journal of Crystal Growth*, vol. 220, pp. 316-325.

Gelfgat, A. Yu.; Bar-Yoseph, P. Z.; Solan, A. (2001): Effect of axial magnetic field on three-dimensional instability of natural convection in a vertical Bridgman growth configuration. *International Journal of Crystal Growth*, vol. 230, pp. 63-72.

Kawaji, M.; Gamache, O.; Hwang, D. H.; Ichikawa, N.; Viola, J. P. et al. (2003): Investigation of Marangoni and natural convection during protein crystal growth. *International Journal of Crystal Growth*, vol. 258, pp. 420-430.

Lage, J. L.; Bejan, A. (1991): The Ra-Pr domain of laminar convection in an enclosure heated from the side. *Numerical Heat Transfer, Part A*, vol. 19, pp. 21-41.

Lappa, M. (2007): Secondary and oscillatory gravitational instabilities in canonical three-dimensional models of crystal growth from the melt. Part 1: Rayleigh-Bénard systems. *Comptes Rendus Mécanique*, vol. 335, pp. 253-260

Lee, Y.; Chun, H. (1999): Transition from regular to irregular thermal wave by coupling of natural convection with rotating flow in Czochralski. *International Journal of Crystal*

Growth, vol. 197, pp. 297-306.

Mahfooz, S. M.; Hossain, M. A. (2012): Conduction-radiation effect on transient natural convection with Thermophoresis. *Applied Mathematics and Mechanics (English Edition)*, vol. 33, pp. 271-288.

Müller, G.; Neumann, G.; Weber, W. (1984): Natural convection in vertical Bridgman configurations. *International Journal of Crystal Growth*, pp. 78-93.

Nakano, A.; Ozoe, H. (1998): Churchill S.W, Numerical computation of natural convection for a low-Prandtl-number fluid in a shallow rectangular region heated from below. *Chemical Engineering Journal*, vol. 71, pp. 175-182.

Nishimura, T.; Wakamatsu, M.; Morega, A. M. (1998): Oscillatory double-diffusive convection in a rectangular enclosure with combined horizontal temperature and concentration gradients. *International Journal of Heat and Mass Transfer*, vol. 41, pp. 1601-1611.

Oueslati, F.; BenBeya, B.; Lili, T. (2014): Numerical investigation of thermosolutal natural convection in a rectangular enclosure of an aspect ratio four with heat and solute sources. *Heat and Mass Transfer*, vol. 50, pp. 721-736.

Patankar, S. V. (1980): *Numerical Heat Transfer and Fluid Flow*. Hemisphere, Washington DC, New York.

Pesso, T.; Piva, S, (2009): Laminar natural convection in a square cavity: Low Prandtl numbers and large density differences. *International Journal of Heat and Mass Transfer*, vol. 52, pp. 1036-1043.

Teamah, M. A. (2008): Numerical simulation of double diffusive natural convection in rectangular enclosure in the presences of magnetic field and heat source. *International Journal of Thermal Sciences*, vol. 47, pp. 237-248.

Uspenskii, V.; Favier, J. J. (1994): High frequency vibration and natural convection in Bridgman-scheme crystal growth. *International Journal of Heat and Mass Transfer*, vol. 37, pp. 691-698.

Yoshio, M.; Akira, S.; Yutaka, M.; Chiaki, Y.; Takao, T. (2009): Numerical simulation of natural convection heat transfer in a ZnO single Crystal Growth hydrothermal autoclave-Effects of fluid properties. *International Journal of Crystal Growth*, vol. 311, pp. 675-679.